GENERAL PHYSICS

I. MOLECULE MICROSCOPY

Academic and Research Staff

Prof. John G. King
Dr. John W. Peterson

Dr. James C. Weaver
Frank J. O'Brien

Graduate Students

H. Frederick Dylla
Joseph A. Jarrell

Steven R. Jost
Dusan G. Lysy

Bruce R. Silver
Peter W. Stevens

A. NEUTRAL-ION RATIO MICROSCOPY

James C. Weaver, H. Frederick Dylla

Recent work[1,2] in the Molecular Beams group has been directed toward developing several types of molecule microscopy. One of these, scanning desorption molecule microscopy (SDMM) using electron-stimulated desorption (ESD) offers particular promise in materials science applications. The basic idea is first to expose a surface to a flux of neutral, surface-stain molecules in such a way that molecules stick in regions of preferred binding and not in others. Subsequently, molecules are desorbed with a scanning electron beam and detected with an ionizer-mass spectrometer in order to reveal where the applied molecules bind. Thus we seek a pictorial mapping of binding sites for neutral molecules, and in so doing utilize surface chemistry interactions (defining the binding sites) to provide contrast.

We propose now neutral-ion ratio microscopy, an extension of this technique which should also provide another form of contrast, one based on electron tunneling (which is itself a convolution of electronic levels), density of states, matrix elements, etc. of the sample surface. Conceptually, the experimental arrangement is simple: surface-stain molecules are desorbed from the sample surface, but the number of neutrals, n^0, and ions, n^+, are detected separately (for example, with a 50% duty cycle). The quantity $(n^0 + n^+)$ provides a measure of the binding-site density while, as we shall argue qualitatively, the ratio n^0/n^+ should depend on surface parameters such as variations in electron tunneling probability, and so forth.

A recent experiment[3] has shown that there is approximately a tenfold intensity variation as a function of desorption (emission) angle for desorbed 0^+ ions (neutrals were not measured) from a clean W (100) surface. This angular variation in desorbed ion intensity is independent of the angle of incident (desorbing) electrons. A possible explanation of this striking experimental result stimulated the idea of Neutral-Ion Ratio Microscopy (NIRM). Although the ESD desorption process is complicated, a simplified qualitative explanation[4-6] can be broken down into the following components: (i) primary
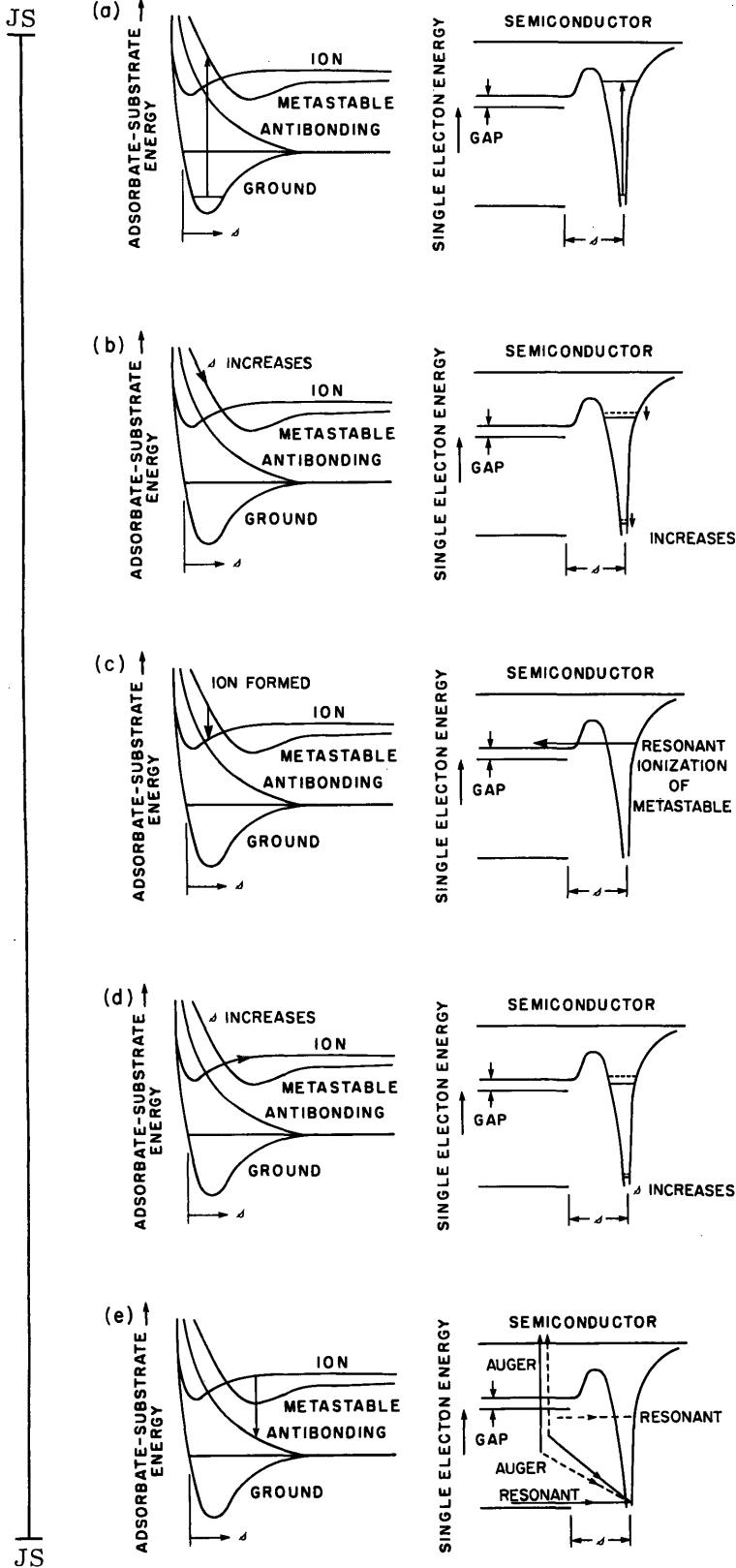
Fig. I-1.

Energy-level diagrams for energy of adsorbate-substrate interaction and for single electrons of the same system, with Δ the adsorbate-substrate separation. A hypothetical desorption process might include: (a) Primary excitation from the adsorbed ground state to a metastable state. (b) Initial outward movement of the metastable curve because, by the Frank-Condon principle, the repulsive part of the metastable curve is reached. As Δ increases the energy levels of the single-electron representation decrease and the adsorbate acquires kinetic energy. (c) Formation of an ion by resonant ionization. (d) Further increase in Δ because, by assumption, sufficient kinetic energy has already been acquired by the outward-moving adsorbate. The single-electron levels decrease further. (e) A neutralizing transition to an antibonding state, with either resonant or Auger processes possible, so that in this hypothetical sequence a desorbed neutral results. It should be emphasized that this hypothetical sequence is intended to represent the variety of possible transitions that govern the desorption of neutrals and ions, and hence the ratio of neutrals to ions.

excitation of the adsorbate-substrate (adsorbed molecule-surface) system by a single incident electron to the repulsive portion of a metastable state, (ii) deexcitation before desorption with high probability (which accounts for the low overall ESD cross sections), but in some cases a transition to either an ionic or a neutral state, including remaining in the metastable state, after sufficient kinetic energy has been accumulated for desorption. For reasons of experimental convenience, most workers have studied only ions, although a few have measured metastable[7] or ground-state neutrals.[8]

As Madey and Yates pointed out in their review,[6] the considerable work on ion neutralization spectroscopy (INS) of Hagstrum and his co-workers[9] should be relevant to understanding the types of transition between the metastable state and the ionic or other electrically neutral states. For example, depending on the electronic states of the surface and the perturbed ionization potential of the molecule, a molecule near a surface may be ionized or an ion neutralized by resonant or Auger electron tunneling processes. Since tunneling processes in general are sensitive to density of states, matrix elements, etc., the ratio n^0/n^+ of desorbed molecules should be sensitive to variations in these properties of the surface. Furthermore, tunneling processes occur readily only over short distances so that n^0/n^+ should mainly be sensitive to the outermost monolayer of the surface. This uniquely high sensitivity to surface rather than bulk properties has been found and emphasized by Hagstrum for INS.

Naively, then, we may think of ESD as an excitation to a primary state followed usually by deexcitation without desorption but occasionally by desorption in which the ratio n^0/n^+ is governed by time-reversed INS. A possible sequence of events is shown in Fig. I-1 where two different approximate representations are used.

By varying the choice of stain molecule, we can hope to vary both the affinity for binding sites (relevant to the $n^0 + n^+$ signal) and the ionization potential (relevant to the n^0/n^+ signal), so that both signals should respond to spatial variations of the sample surface. Again speaking simply, the application of SDMM with ESD should provide contrast with surface specificity revealing variations in the chemical nature of the surface (binding site distribution by $n^0 + n^+$) and, in a complicated way, in the electronic surface properties (via n^0/n^+). We are beginning experiments in which two materials (gold and carbon) are deposited to provide a test surface with large-scale (10^{-1} cm) spatial variation in composition, and we shall examine both $n^0 + n^+$ and n^0/n^+ signals in order to see if the expected contrast exists.

Stimulating conversations with P. W. Stephens and J. G. King are gratefully acknowledged.

References

1. J. C. Weaver and J. G. King, Proc. Natl. Acad. Sci. U.S. 70, 2781 (1973).

2. J. C. Weaver, Quarterly Progress Report No. 113, Research Laboratory of Electronics, M. I. T., April 15, 1974, pp. 1-7; H. F. Dylla and G. A. Herzlinger, Quarterly Progress Report No. 108, Research Laboratory of Electronics, M. I. T., January 15, 1973, pp. 2-5.

3. J. J. Czyzewski, T. E. Madey, and J. T. Yates, Phys. Rev. Letters 32, 777 (1974).

4. P. A. Redhead, Can. J. Phys. 42, 886 (1964).

5. D. Menzel and R. Gomer, J. Chem. Phys. 41, 3311 (1964).

6. T. E. Madey and J. T. Yates, J. Vac. Sci. Technol. 8, 525 (1971).

7. I. G. Newsham, J. V. Hogue, and D. R. Sandstrom, J. Vac. Sci. Technol. 9, 596 (1972).

8. D. Menzel, Ber. Bunsenges. Physik. Chem. 72, 591 (1968).

9. H. D. Hagstrum, Science 178, 275 (1972).

B. TRANSMISSION-RESOLUTION CURVES FOR THE QUADRUPOLE MASS SPECTROMETER

H. Frederick Dylla, Joseph A. Jarrell

The electric quadrupole mass filter developed by Paul et al.[1] has recently become the basis of an important piece of laboratory instrumentation[2] and is now available from numerous manufacturers of commercial mass spectrometer systems. An important measure of the performance of a quadrupole mass filter as a mass spectrometer is obtained as a plot of the transmission through the quadrupole for ions of a particular mass m as a function of the resolving power $m/\Delta m$, where Δm is the half-width of the mass line.

According to the usual trade-off in mass spectrometers, the resolution increases with decreasing transmission. The transmission-resolution curve for a quadrupole mass spectrometer is characterized by two regions of differing slope. In the first region of the curve, near unity relative transmission, the decrease in transmission with resolution is small. A figure of merit obtained from the curve in this region is the highest attainable resolution at near unity transmission. Theoretically, this number depends on the size of the entrance aperture relative to the size of the quadrupole (or the effective size of the aperture if ion lenses are employed to focus the entering ion beam), and on the transverse momentum of the ions relative to the applied quadrupole voltages.[3] The mass peaks in this region have flat-topped trapezoidal shapes.

In the second region of the curve, the decrease in transmission with increasing resolution is much more drastic. In this region, a figure of merit is the ultimate resolution obtained from a distinguishable mass line and the relative transmission at this point.
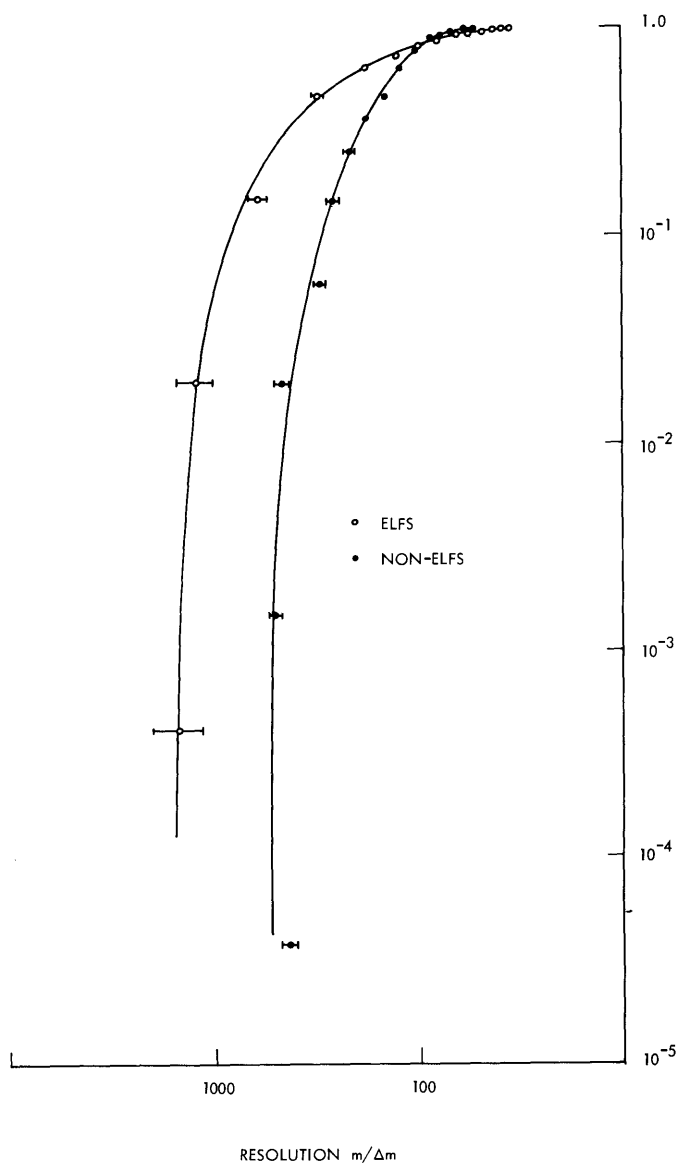
RELATIVE TRANSMISSION

∘ ELFS

• NON-ELFS

10^{-1}

10^{-2}

10^{-3}

10^{-4}

10^{-5}

1.0

1000   100

RESOLUTION m/Δm

Fig. I-2.

Relative transmission vs reso-
lution for the 28 amu peak. Data
relevant to the mass spectrom-
eter operation for these curves:
emission current = 33 mA, elec-
tron energy = 100 V, ion energy
= +7 V, extractor voltage = +7 V,
ion lens #1 = +4 V, ion lens #2 =
+4 V, ion lens #3 = -68 V, ΔM
(half-width) control = 0 V, elec-
tron multiplier voltage = -4 kV,
electron multiplier gain = 1.5 ×
10^{4}. For the ELFS curve P_{N_2} = 1.5

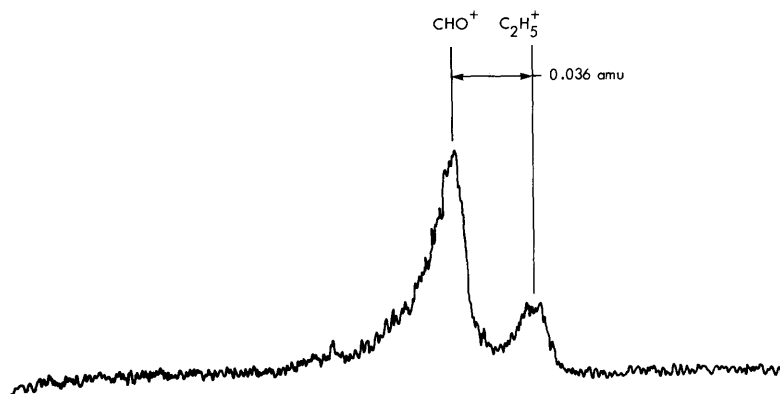× 10^{-6} Torr; for the non-ELFS

curve P_{N_2} = 4.7 × 10^{-6} Torr.

CHO^{+} $C_2H_5^{+}$

0.036 amu

Fig. I-3.

Best resolved multiple peak
(29 amu) with ELFS quadru-
pole.

JS

JS

As in the first region, this figure of merit depends theoretically on the entrance conditions; the ultimate resolution can also be limited by the precision of the quadrupole dimensions and applied voltages.[4] The mass peaks in this region have triangular shapes.

We have measured the transmission-resolution curve for a quadrupole mass spectrometer that was one of several purchased from Extranuclear Laboratories,[5] for the purpose of molecular-beam detection and residual gas analysis. The transmission resolution curves were measured with and without a design change for the quadrupole entrance aperture that has recently been developed by Extranuclear Laboratories. The new design has been designated ELFS (Extranuclear Laboratories Field Separation) and patents are pending. We have confirmed that the design change improves the resolution at near unity transmission and the ultimate attainable resolution.

1. Experimental Apparatus

The quadrupole (#324-9) had a field radius of .95 cm, a length of 22 cm, and was operated at a frequency of 3.7 MHz for a nominal mass range of 0-32 amu by the Extranuclear Laboratories power system (#011-1B). An axial electron bombardment ionizer (#041-1) and an off-axis 14-stage Cu-Be electron multiplier (EMI 9603B) were used with the quadrupole. The output current of the electron multiplier was detected with a FET operational amplifier (AD 540J) and displayed on a strip chart recorder or storage oscilloscope. The entire quadrupole assembly was flange-mounted in a 70-liter stainless-steel, Viton and lead O-ring sealed, vacuum system. The vacuum system was pumped by a liquid nitrogen trapped Varian NHS-4 diffusion pump with DC 705 as the pump fluid.

2. Procedure and Results

Measurements were made with the vacuum system containing a partial pressure of N_2 in the 10^{-6} Torr range as determined by a nude Bayard-Alpert gauge. The ionizer and quadrupole electronics were adjusted for maximum transmission and a smooth trapezoidal shape for the 28 amu peak, with a resolution that just resolved the peak from the adjacent 27 amu and 29 amu peaks. The height and half-width of this peak established the point of unity transmission and minimum resolution on the transmission-resolution curve. The resolution was incrementally increased subsequently and the corresponding trace of the 28 amu peak was recorded on the strip chart recorder and oscilloscope.

The procedure was repeated with the ELFS entrance aperture in place of the usual grounded entrance aperture. Relative transmission vs resolution of the 28 amu peak is plotted in Fig. I-2 for the ELFS and non-ELFS quadrupoles. The plot shows that both

JS quadrupoles are capable of resolving adjacent mass peaks over the entire mass range

with near unity transmission ($m/\Delta m \approx 70$ at a relative transmission of .90). It also shows that the ELFS quadrupole attains a significantly greater resolution than the non-ELFS quadrupole for all values of relative transmission below the trapezoidal peak (near unity transmission) region. The ultimate attainable resolution for ELFS is 1500, compared with 500 for the non-ELFS.

Figure I-3 shows a tracing of the best resolved multiple peak (29 amu) in the background spectrum that was obtained with the ELFS quadrupole. With the 29 amu doublet identified as CHO^+-$C_2H_5^+$ after Fite and Irving,[6] the resolved mass difference is .036 amu. We were unable to split the 28 amu peak into its three constituents (N_2^+, CO^+, $C_2H_4^+$) during our measurements, since this would have required a resolvable mass difference of the order of .010 (or $m/\Delta m \approx 3000$).

Oscilloscope traces showing the peak shapes obtained for the first 11 points of the transmission-resolution curve are shown in Fig. I-4a for the ELFS quadrupole and in

ELFS

QUADRUPOLE

4.5×10^{-4} A/Torr N_2^*

0.2 amu/cm

(a)

NON-ELFS

QUADRUPOLE

3.3×10^{-5} A/Torr N_2^*

0.2 amu/cm

(b)
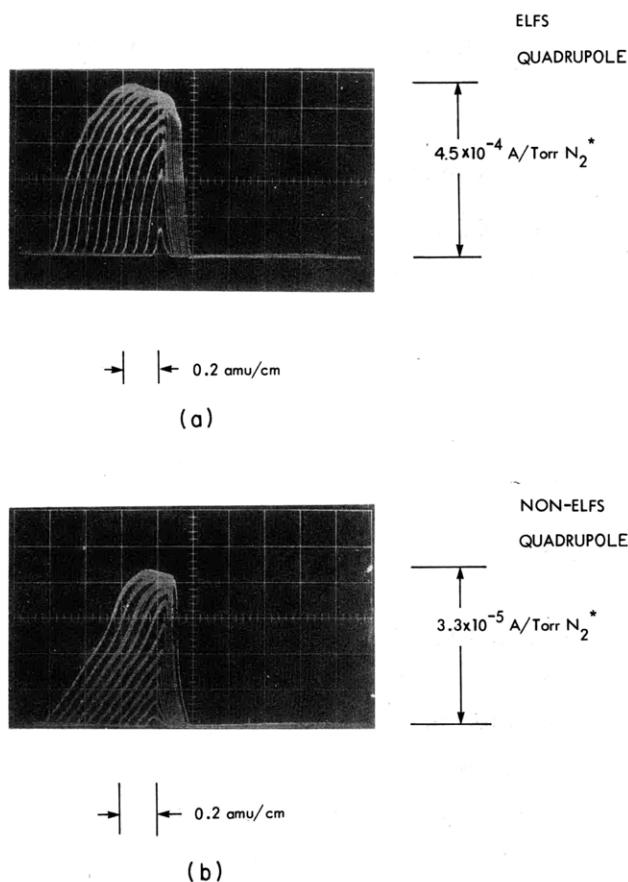
* ION CURRENT AT THE INPUT OF THE ELECTRON MULTIPLIER

Fig. I-4. Mass 28 peak shape for transmission vs resolution data of Fig. I-2.

JS

Fig. I-4b for the non-ELFS quadrupole. The ordinate of Fig. I-4a gives the approximate absolute transmission for background gas (in A/Torr N_2 before electron multiplier gain) based on the ion gauge pressure measurement. Note that the absolute sensitivity of the ELFS quadrupole is an order of magnitude larger than that of the non-ELFS.

References

1. W. Paul and H. Steinwedel, Z. Naturforsch. 8A, 448 (1953); W. Paul and M. Raether, Z. Physik 140, 262 (1955).

2. For a recent review see P. H. Dawson and N. R. Whetten, "The Monopole Mass Spectrometer," Advances in Electronics and Electron Physics (Academic Press, Inc., New York, 1969), Vol. 21, pp. 59-90.

3. Ibid., p. 88.

4. Ibid., p. 89.

5. The quadrupole mass spectrometer manufactured by Extranuclear Laboratories, Inc. was chosen as the result of a comparative study of 9 commercially available instruments, Internal Report, Molecular Beam Laboratory, Research Laboratory of Electronics, M. I. T., October 25, 1972.

JS
6. W. L. Fite and P. Irving, J. Vac. Sci. Technol. 11, 351 (1974).

C. ASSAY BY VOLATILE ENZYME PRODUCTS

James C. Weaver

During the past year we have developed plans for a highly sensitive biochemical assay. The technique is based on the detection of volatile enzyme products (VEP), and thereby combines enzyme specificity and the ability to count individual molecules in a vacuum system with an expected efficiency $\epsilon_T \approx 10^{-4}$. One basic configuration is shown in Fig. I-5.

The potential sensitivity and time response of the VEP technique can be estimated in the following way. Three effective permeabilities act in series to determine the rate at which a nonvolatile substrate, S, is converted into a flux of neutral molecules in the vacuum system. The first is the diffusion of S through the unstirred layer. The second is the enzyme, E, reaction rate for the conversion of S into products, at least one of which must be a volatile, V, and must also be permeable to the membrane. The third is the permeability of the membrane. If D_S is the substrate diffusion constant, the first effective permeability is $D_S/x \approx 10^{-3}-10^{-4}$ cm-s^{-1}. Also, if the amount of immobilized enzyme is expressed as the number of monolayers, n_{mL}, and $\sigma_E \approx 10^{12}$ molecules E-cm^2 is the monolayer density, then the effective permeability is
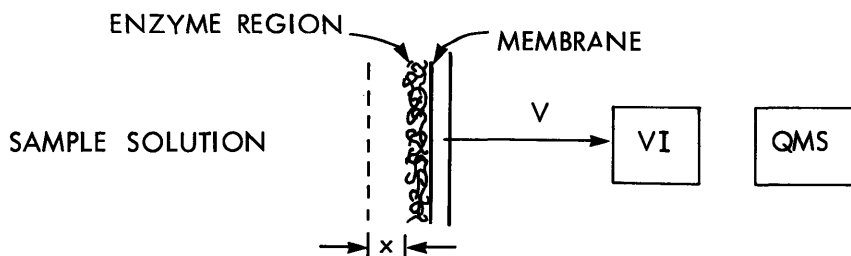
Fig. I-5. Schematic of a VEP configuration. The sample molecules are the substrate, S, for the enzyme which is immobilized near or on one side of a semipermeable membrane. An unstirred boundary layer of thickness $\sim 10^{-2}$ cm presents a diffusive barrier to S, and, in many cases, also serves to keep most of the volatile product from diffusing back into the sample solution, since the membrane permeability, P_M, can be much greater than D_v/x, where D_v is the volatile's diffusion constant. If the membrane area ≈ 1 cm^2 and a minimum count rate of $\dot{n} = 1$ cps is taken to represent an ultimate limit of detectability, then the corresponding minimum detectable substrate concentration is estimated to be $[S]_{min} \approx 5 \times 10^{-14}$ M for systems for which a suitable enzyme and volatile product can be obtained. Here UI is a universal ionizer and QMS is a quadrupole mass spectrometer for detection and identification of the volatile products.

$$\frac{V_m}{K_m} = \frac{n_m L^{\sigma} E^{\nu} T^f l}{K_m},$$

where ν_T is the turnover number in molecules S per molecule E per second, f_l is the fraction of active enzyme, and K_m is the Michaelis constant. Depending on the type of immobilization and the enzyme reaction that is used, the range $10^{-4} \lesssim V_m/K_m \lesssim 10^1$ cm-s^{-1} is expected. Finally, by suitable choice, the membrane permeability can be $P_M \approx 10^{-2}$ cm. Thus, the total effective permeability is determined from

$$P_{eff}^{-1} = \left(\frac{D_S}{x}\right)^{-1} + \left(\frac{V_m}{K_m}\right)^{-1} + P_M^{-1}$$

and typically will be in the range $10^{-4} \lesssim P_{eff} \lesssim 10^{-3}$ cm-s^{-1}. Of the volatile products generated, a fraction, $P_M/[P_M+D_v/x]$, will permeate the membrane and evaporate into the vacuum. The technical problems of detecting small fluxes of neutral molecules in vacuum are identical to those encountered in molecule microscopy. We expect the total counting efficiency, ϵ_T, to be $\epsilon_T = \epsilon(\Omega/\pi)$, where $\epsilon \approx 10^{-3}$ is the universal ionizer efficiency, and Ω/π is the solid angle fraction for effusion which is subtended by the ionizer. Finally, if the membrane area is A_m, the expected count rate is

$$\dot{n}_S \approx \left\{ P_{eff} \left[\frac{P_M}{P_M + (P_v/x)} \right] A_m \epsilon \left(\frac{\Omega}{\pi} \right) \right\} [S],$$

where $[S]$ is the substrate concentration in molecules-cm^{-3}.

The time response of the VEP technique should usually be limited by the substrate diffusion time, $\tau_D \approx x^2/2D \approx 10$ s. Thus, for example, at a concentration $[S] = 10^{-12}$ $\underline{M}$ the expected count rate is ~2×10^1 with an accumulated count in 10 s to get a signal-to-noise ratio of ~15.

In another configuration it should be possible to react all of the sbustrate and, furthermore, to arrange for all of the product to permeate the membrane into the vacuum. With the same criterion in this mode the ultimate limit of detectability should be ~10^{-20} mole or 10^4 molecules.

Preliminary experiments in collaboration with M. K. Mason and J. A. Jarrell are in progress and are yielding very encouraging results which suggest that the high expected sensitivity will be realized. The author also acknowledges helpful conversations with J. W. Peterson, Professor C. L. Cooney, of the Department of Nutrition, M. I. T., and J. G. King.